# BBN
# Status and perspectives

Ofelia Pisanti

Università di Napoli Federico II and INFN Napoli

Theoretical Astroparticle Group – Department of Physics E. Pancini

GIANTS XI – 20-21 October 2022

# Summary

- BBN in brief
- The quest for precision: theory vs data
- S-factor analysis and results
- Cosmological analysis
- Non standard scenarios
- Conclusions

# BBN in brief

1. Less than 1 second after the bang, the plasma of γ $e^-$, ν, n, p (and their antiparticles) is in equilibrium.
2. At T~1 MeV (1 second) neutrinos decouple because their weak interactions go out of equilibrium with respect to expansion.
3. n/p ratio (fortunately) freezes out just soon after neutrinos, at $T_D$~800 keV; then, when a sufficient abundance of deuterium forms at $T_{BBN}$~100 keV, the nuclear chain starts: (almost) all neutrons present at this moment go into $^4$He.

The final result is a universe made by 75% of hydrogen, 25% of $^4$He (and negligible yields of the other elements up to $^7$Li).

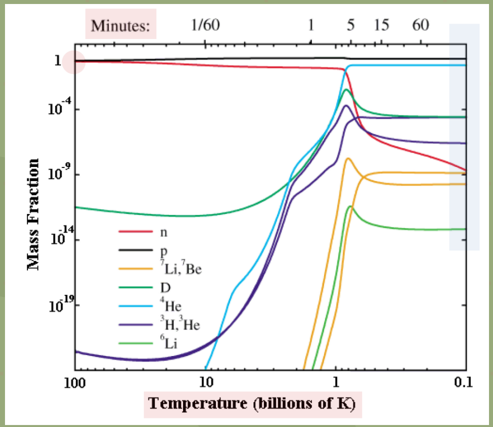


mass fraction of $^4$He in a simple equation

$$Y_p = \frac{4\, n_{^4He}}{n_n + n_p} = \frac{4\ n_n/2}{n_n + n_p} = \frac{2}{1 + n_p/n_n} = 0.25$$

# BBN in brief

cosmological model
weak rates
nuclear rates…

→ code → Nuclide abundances

In the standard minimal model the only free parameter is the baryon to photon number density: $\eta_b = \frac{n_b}{n_\gamma} = 273.45 \cdot 10^{-10} \Omega_b h^2$

R.V. Wagoner, Astrophys. J. Suppl. 18 (1969) 247
R.V. Wagoner, Astrophys. J. 179 (1973) 343

L.H. Kawano, 1988. Preprint FERMILAB-Pub-88=34-A
L.H. Kawano, 1992. Preprint FERMILAB-Pub-92=04-A

R.E. Lopez, M.S. Turner, Phys. Rev. D 59 (1999) 103502
…

E. Lisi, S. Sarkar, F.L. Villante, Phys. Rev. D 59 (1999) 123520

K.A. Olive, G. Steigman, T.P. Walker, Phys. Rep. 333334 (2000) 389

S. Esposito, G. Mangano, G. Miele, O. Pisanti, JHEP 0009 (2000) 038
P.D. Serpico, et al., JCAP 0412 (2004) 010

PArthENoPE: O. Pisanti et al., Comp. Phys. Comm. 178 (2008) 956; Comp. Phys. Comm. 233 (2018) 237

AlterBBN: A. Arbey, Comp. Phys. Comm. 183 (2012) 1822

PRIMAT: C. Pitrou, A. Coc, J.-P. Uzan, E. Vangioni, Phys. Rep. 754 (2018) 1

PArthENoPE3.0

S. Gariazzo, P.F. de Salas, O. Pisanti, R. Consiglio,
*Comput.Phys.Commun.* (2022) 108205, 271

# The quest for precision: theory vs data

Accuracy of primordial elements abundances measurement. Indirect observations, since stars have changed the chemical composition of the universe. Strategies are observation in "primordial" systems or careful account for chemical evolution: increasingly precise astrophysical data on D (1%), He measured by different groups with less than 1.5% accuracy but one determination is at 4% distance, the situation is not clear for Li (the value is a factor 2-3 below the BBN prediction, lithium depletion problem).

→ **systematics and astrophysical evolution**

Accuracy of the BBN codes. Standard physics, theoretical framework well established, but outputs of the nuclear network depend on the determination of several critical reactions. In the past mainly experimental measures (not always in the relevant energy range for BBN, 10÷400 keV in the center of mass), now also theoretical calculations.

→ **nuclear reaction data and analysis methods**

# Astrophysical data

- $^2$H: it is only destroyed. Observation of Lyman absorption lines by neutral H and D (HI, DI) gas clouds (Damped Lyman-$\alpha$, DLAs) at red-shift $z \approx 2 - 3$ placed along the line of sight of distant quasar. Few systems, but next generation 30-m class telescopes will increase the number.
- $^3$He: in stellar interior can be either produced by $^2$H-burning or destroyed in the hotter regions. It was observed only within Milky Way and magnitude and sign of the correction for the contamination by ejecta from earlier generation of stars are uncertain. Next generation 30-m class telescopes may measure $^3$He/$^4$He.
- $^4$He: it is produced inside stars. Observation in ionized gas regions (HeII → HeI recombination lines) in low metallicity environments (BCG or dwarf irregular), with O abundances 0.02 – 0.2 times those in the sun. Then, regression to zero metallicity. Large systematics (1% accuracy at best), but CMB allows interesting measure via $^4$He effect on acoustic peak tail.
- $^7$Li: it is produced (BBN and spallation) and destroyed. Observation of absorption lines in spectra of halo stars of POP II. Spite plateau at medium metallicity, but scattered points at low metallicity. The experimental value is a factor 2-3 below the BBN prediction. Attempts at solutions: nuclear rates, stellar depletion, new particles decaying at BBN, axion cooling, variation of fundamental constants. However, a measure from the Small Magellanic Cloud is at BBN level.

# Theory inputs

Aghanim et al., Planck 2018

- baryon to photon number density

$$\eta_b = \frac{n_b}{n_\gamma} = 273.45 \cdot 10^{-10} \Omega_b h^2$$

# Theory inputs

Aghanim et al., Planck 2018

- baryon to photon number density

$$\eta_b = \frac{n_b}{n_\gamma} = 273.45 \cdot 10^{-10} \Omega_b h^2$$

Bennett et al., JCAP 04 (2021) 073

- energy density in relativistic degrees of freedom

$$\rho_R = \rho_\gamma + \rho_\nu = \rho_\gamma + \rho_\gamma \frac{7}{8} 3.045 \left(\frac{4}{11}\right)^{4/3} + \rho_\gamma \Delta N_{eff} \frac{7}{8}\left(\frac{4}{11}\right)^{4/3}$$

photons

standard neutrinos

new physics

# Theory inputs

Aghanim et al., Planck 2018

- baryon to photon number density

$$\eta_b = \frac{n_b}{n_\gamma} = 273.45 \cdot 10^{-10} \Omega_b h^2$$

- weak rates (main input for $Y_p$)

1. radiative corrections $O(\alpha)$
2. finite nucleon mass corrections $O(T/m_N)$
3. plasma effects $O(\alpha\, T/m_e)$

Esposito et al., Nucl.Phys. B540 (1999) 3

Bennett et al., JCAP 04 (2021) 073

- energy density in relativistic degrees of freedom

$$\rho_R = \rho_\gamma + \rho_\nu = \rho_\gamma + \rho_\gamma \frac{7}{8}\, 3.045 \left(\frac{4}{11}\right)^{4/3} + \rho_\gamma\, \Delta N_{eff} \frac{7}{8}\left(\frac{4}{11}\right)^{4/3}$$

photons

standard neutrinos

new physics

# Theory inputs

Aghanim et al., Planck 2018

- baryon to photon number density

$$\eta_b = \frac{n_b}{n_\gamma} = 273.45 \cdot 10^{-10} \Omega_b h^2$$

- weak rates (main input for $Y_p$)

1. radiative corrections $O(\alpha)$
2. finite nucleon mass corrections $O(T/m_N)$
3. plasma effects $O(\alpha\ T/m_e)$

Esposito et al., Nucl.Phys. B540 (1999) 3

Bennett et al., JCAP 04 (2021) 073

- energy density in relativistic degrees of freedom

$$\rho_R = \rho_\gamma + \rho_\nu = \rho_\gamma + \rho_\gamma \frac{7}{8}\, 3.045 \left(\frac{4}{11}\right)^{4/3} + \rho_\gamma \Delta N_{eff} \frac{7}{8}\left(\frac{4}{11}\right)^{4/3}$$

photons

standard neutrinos

new physics

- nuclear rates

Mossa et al., Nature 587 (2020) 7833, 210

1. more precise data on nuclear cross sections (ex.: LUNA measure of $d(p,\gamma)\ ^3He$)
2. «ab initio» nuclear theoretical calculations (ex.: DD reactions)

Viviani et al., e-Print: 2207.01433

$$\langle \sigma v \rangle = \sqrt{\frac{8}{\pi \mu_{ab}}} T^{-3/2} \int_0^\infty \mathrm{d}E\, E\, \sigma(E)\, \mathrm{e}^{-E/T}$$

$$S(E) = \sigma(E) E\, e^{\sqrt{E_G/E}}$$

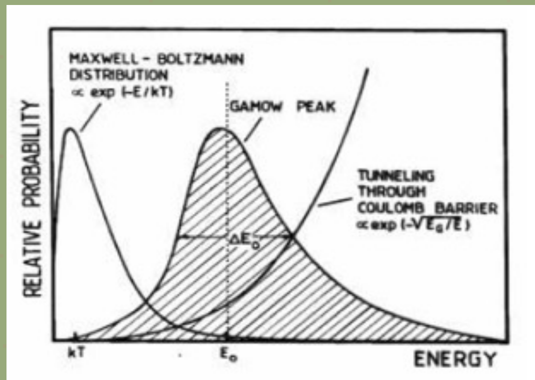

# Outstanding results from LUNA

Deuterium synthesis

| Symbol | Reaction | Symbol | Reaction |
|---|---|---|---|
| $R_0$ | $\tau_n$ | $R_8$ | $^3\mathrm{He}(\alpha,\gamma)^7\mathrm{Be}$ |
| $R_1$ | $p(n,\gamma)d$ | $R_9$ | $^3\mathrm{H}(\alpha,\gamma)^7\mathrm{Li}$ |
| $R_2$ | $\boxed{^2\mathrm{H}(p,\gamma)^3\mathrm{He}}$ | $R_{10}$ | $^7\mathrm{Be}(n,p)^7\mathrm{Li}$ |
| $R_3$ | $\boxed{^2\mathrm{H}(d,n)^3\mathrm{He}}$ | $R_{11}$ | $^7\mathrm{Li}(p,\alpha)^4\mathrm{He}$ |
| $R_4$ | $\boxed{^2\mathrm{H}(d,p)^3\mathrm{H}}$ | $R_{12}$ | $^4\mathrm{He}(d,\gamma)^6\mathrm{Li}$ |
| $R_5$ | $^3\mathrm{He}(n,p)^3\mathrm{H}$ | $R_{13}$ | $^6\mathrm{Li}(p,\alpha)^3\mathrm{He}$ |
| $R_6$ | $^3\mathrm{H}(d,n)^4\mathrm{He}$ | $R_{14}$ | $^7\mathrm{Be}(n,\alpha)^4\mathrm{He}$ |
| $R_7$ | $^3\mathrm{He}(d,p)^4\mathrm{He}$ | $R_{15}$ | $^7\mathrm{Be}(d,p)2\,^4\mathrm{He}$ |

Di Valentino et al., Phys. Rev. D90 (2014) no. 2, 023543

## before LUNA

| Reaction | Rate symbol | $\sigma_{^2\mathrm{H/H}} \times 10^5$ |
|---|---|---|
| $p(n,\gamma)^2\mathrm{H}$ | $R_1$ | $\pm 0.002$ |
| $d(p,\gamma)^3\mathrm{He}$ | $R_2$ | $\pm 0.062$ |
| $d(d,n)^3\mathrm{He}$ | $R_3$ | $\pm 0.020$ |
| $d(d,p)^3\mathrm{H}$ | $R_4$ | $\pm 0.013$ |

0.1%
87%
9%
3.8%

- previous data were scarce in the BBN range with ~ 9% uncertainty
- phenomenological fit by Adelberger et al. (AD2011, orange line and band)
- *ab initio* theoretical prediction by Marcucci et al. (2005) updated in 2016 (green line), 15% higher than AD2011
- Bayesian analysis by Iliadis et al. (2016, red line)

## after LUNA

Mossa et al., Nature 587 (2020) 7833, 210

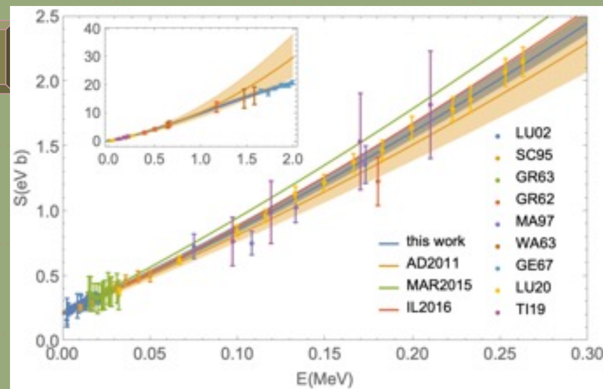


- very precise data (yellow points), $\Delta S/S \leq 2.6\%$, in [30,300] keV $E_{cm}$
- S-factor global fit (dominated by LUNA data) with 3rd order polynomial, $\chi_{red}^2 = 1.02$ (blue line and band)

# Cosmological analysis

- Choose the scenario, that is the parameters of your model: A, B, ….
- Run your favourite BBN code and determine the theoretical abundances $X_i(A,B,\ldots)$ with corresponding uncertainties $\sigma_i(A,B,\ldots)$.
- Construct likelihood functions for your abundances and determine CL contours corresponding to given experimental measures:

$$L_i(N_{eff},\eta)=\frac{1}{2\pi\sigma_i^{th}(N_{eff},\eta)\sigma_i^{ex}}\int dx\exp\left(-\frac{(x-Y_i^{th}(N_{eff},\eta))^2}{2\sigma_i^{th}(N_{eff},\eta)^2}\right)\exp\left(-\frac{(x-Y_i^{ex})^2}{2\sigma_i^{2x}}\right)$$

# Cosmological analysis

- Choose the scenario, that is the parameters of your model: A, B, ….
- Run your favourite BBN code and determine the theoretical abundances $X_i$(A,B,…) with corresponding uncertainties $\sigma_i$(A,B,…).
- Construct likelihood functions for your abundances and determine CL contours corresponding to given experimental measures:

$$L_i(N_{eff},\eta) = \frac{1}{2\pi\sigma_i^{th}(N_{eff},\eta)\sigma_i^{ex}} \int dx \exp\left(-\frac{(x - Y_i^{th}(N_{eff},\eta))^2}{2\sigma_i^{th}(N_{eff},\eta)^2}\right) \exp\left(-\frac{(x - Y_i^{ex})^2}{2\sigma_i^{2x}}\right)$$

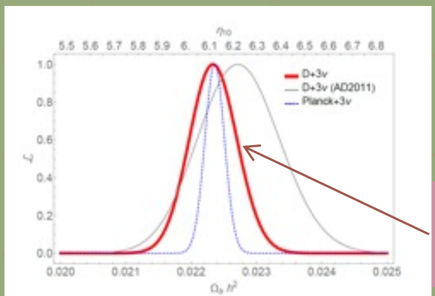


For $N_{eff}$=3.045, $^2$H alone is an efficient baryometer

# Cosmological analysis

- Choose the scenario, that is the parameters of your model: A, B, ….
- Run your favourite BBN code and determine the theoretical abundances $X_i$(A,B,…) with corresponding uncertainties $\sigma_i$(A,B,…).
- Construct likelihood functions for your abundances and determine CL contours corresponding to given experimental measures:

$$L_i(N_{eff},\eta) = \frac{1}{2\pi\sigma_i^{th}(N_{eff},\eta)\sigma_i^{ex}} \int dx \exp\left(-\frac{(x - Y_i^{th}(N_{eff},\eta))^2}{2\sigma_i^{th}(N_{eff},\eta)^2}\right) \exp\left(-\frac{(x - Y_i^{ex})^2}{2\sigma_i^{2x}}\right)$$

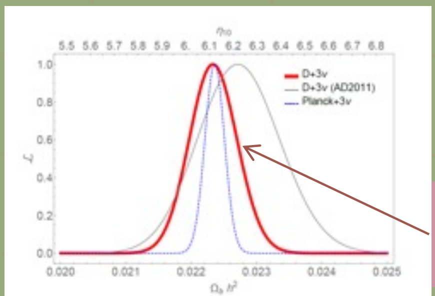


For $N_{eff}$=3.045, $^2$H alone is an efficient baryometer

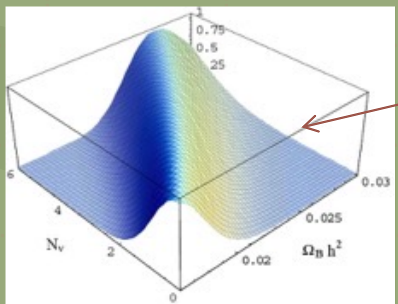


For free $N_{eff}$, $^2$H alone is not sufficient in breaking the degeneracy…

# Cosmological analysis

- Choose the scenario, that is the parameters of your model: A, B, ….
- Run your favourite BBN code and determine the theoretical abundances $X_i(A,B,\ldots)$ with corresponding uncertainties $\sigma_i(A,B,\ldots)$.
- Construct likelihood functions for your abundances and determine CL contours corresponding to given experimental measures:

$$L_i(N_{eff},\eta)=\frac{1}{2\pi\sigma_i^{th}(N_{eff},\eta)\sigma_i^{ex}}\int dx\exp\left(-\frac{(x-Y_i^{th}(N_{eff},\eta))^2}{2\sigma_i^{th}(N_{eff},\eta)^2}\right)\exp\left(-\frac{(x-Y_i^{ex})^2}{2\sigma_i^{2x}}\right)$$

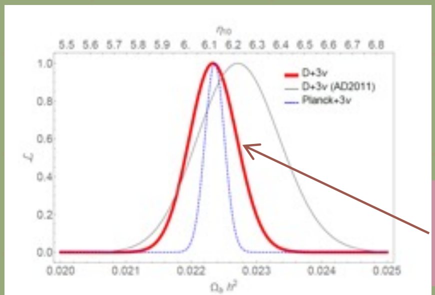

For $N_{eff}$=3.045, $^2$H alone is an efficient baryometer

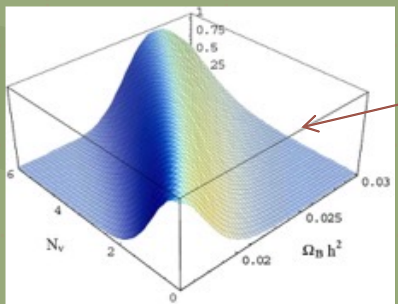

For free $N_{eff}$, $^2$H alone is not sufficient in breaking the degeneracy…

… and you need to add another observable (e.g. $^4$He) or a prior (e.g. $\Omega_b$ Planck)

$^2$H mainly fixes $\Omega_B h^2$, $^4$He depends strongly on $N_{eff}$

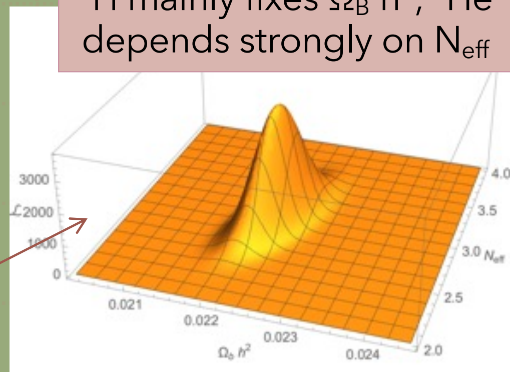

# Cosmological analysis

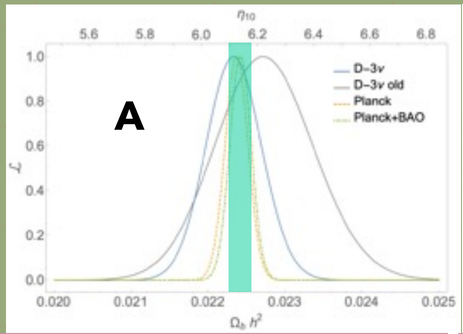


O.P. et al, JCAP 04 (2021) 020

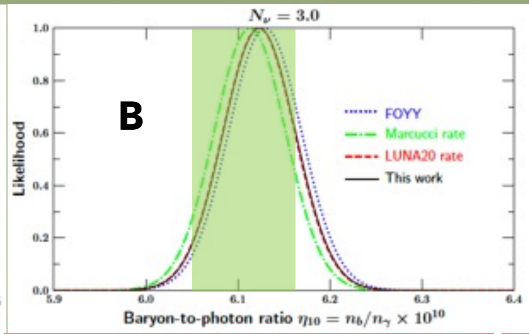


Yeh et al., JCAP 03 (2021) 046

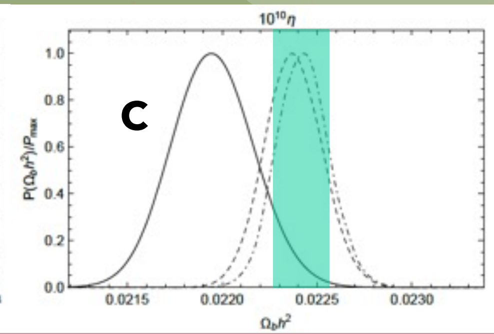


Pitrou et al., M.N.R.Astr.Soc. 502 (2021) 2, 2474

- A(blue) and B(black) in fair agreement with each other and with Planck (1σ green bands)
- C(solid) shows 1.84σ tension with Planck
- Likelihoods come from:
  - ✓ A: only $D_{BBN}$, D/H=2.527±0.030
  - ✓ B: $D_{BBN}$+ $Y_{pBBN}$+CMB, D/H=2.55±0.03, $Y_p$=0.2453+-0.0034
  - ✓ C: $D_{BBN}$+ $Y_{pBBN}$, D/H=2.527±0.030, $Y_p$=0.2453+-0.0034
- Planck green bands correspond to:
  - ✓ A: Planck +$Y_p(\omega_b)$ + lensing + BAO
  - ✓ B: Planck + lensing
  - ✓ C: Planck +$Y_p(\omega_b)$ + lensing + BAO

# Cosmological analysis

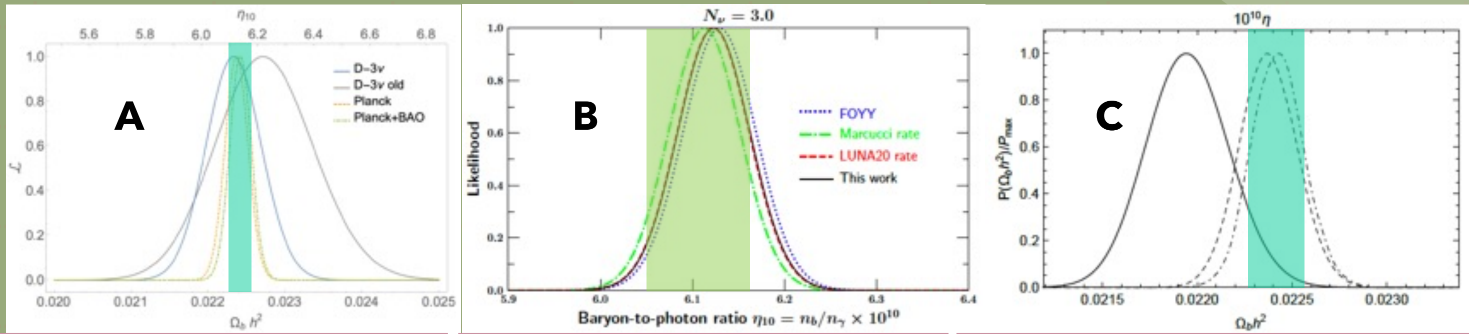


O.P. et al, JCAP 04 (2021) 020 | Yeh et al., JCAP 03 (2021) 046 | Pitrou et al., M.N.R.Astr.Soc. 502 (2021) 2, 2474

- A(blue) and B(black) in fair agreement with each other and with Planck (1σ green bands)
- C(solid) shows 1.84σ tension with Planck
- Likelihoods come from:
  - ✓ A: only $D_{BBN}$, D/H=2.527±0.030
  - ✓ B: $D_{BBN}$+ $Y_{pBBN}$+CMB, D/H=2.55±0.03, $Y_p$=0.2453+-0.0034
  - ✓ C: $D_{BBN}$+ $Y_{pBBN}$, D/H=2.527±0.030, $Y_p$=0.2453+-0.0034
- Planck green bands correspond to:
  - ✓ A: Planck +$Y_p(\omega_b)$ + lensing + BAO
  - ✓ B: Planck + lensing
  - ✓ C: Planck +$Y_p(\omega_b)$ + lensing + BAO

SCM in good shape!

# Cosmological analysis

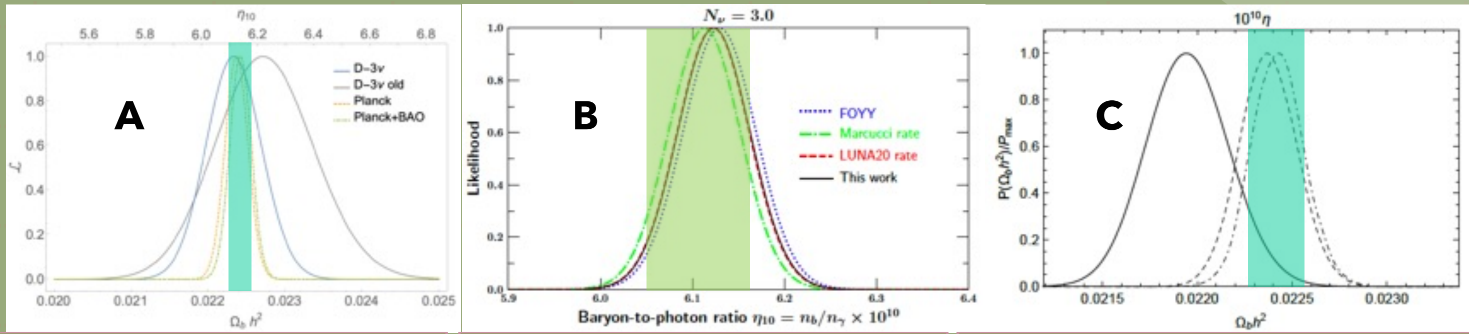


O.P. et al, JCAP 04 (2021) 020 | Yeh et al., JCAP 03 (2021) 046 | Pitrou et al., M.N.R.Astr.Soc. 502 (2021) 2, 2474

- A(blue) and B(black) in fair agreement with each other and with Planck (1σ green b )
- C(solid) shows 1.84σ tension with Planck
- Likelihoods come from:
  - ✓ A: only $D_{BBN}$, D/H=2.527±0.030
  - ✓ B: $D_{BBN}$+ $Y_{pBBN}$+CMB, D/H=2.55±0.03, $Y_p$=0.2453+-0.0034
  - ✓ C: $D_{BBN}$+ $Y_{pBBN}$, D/H=2.527±0.030, $Y_p$=0.2453+-0.0034
- Planck green bands correspond to:
  - ✓ A: Planck +$Y_p(\omega_b)$ + lensing + BAO
  - ✓ B: Planck + lensing
  - ✓ C: Planck +$Y_p(\omega_b)$ + lensing + BAO

tension in SCM!

# The next goal: D+D S-factor measure

Different analyses agree on the fact that the origin of the discrepancy is in the different determinations of the D+D reaction rates. Exercise: which improvement can we foresee by assuming the same precision of LUNA in the D+D rate determination?

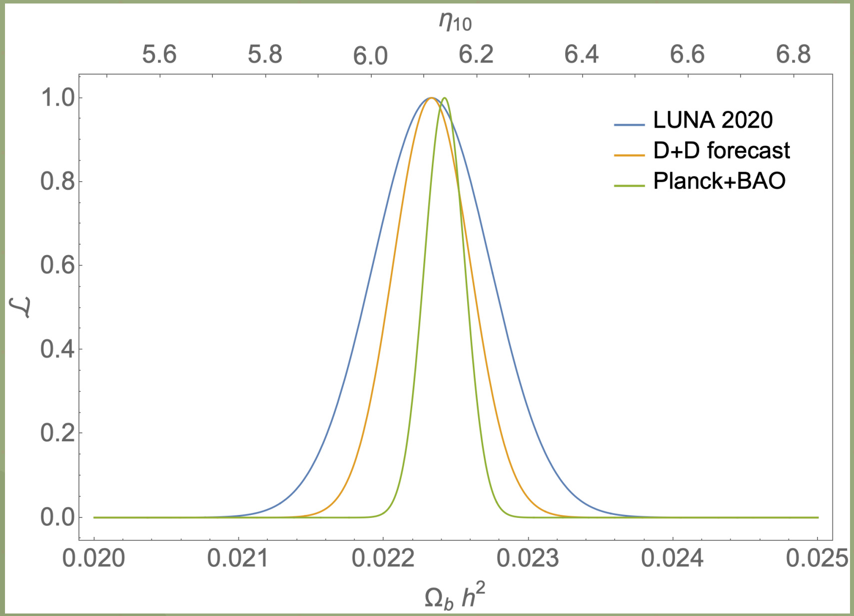


| | $\Delta\Omega_B h^2$ |
|---|---|
| LUNA 2020 | 0.00043 |
| D+D forecast | 0.00026 |
| Planck+BAO | 0.00014 |

# Not standard scenarios

BBN is a powerful «cosmological probe» and can test more exotic scenarios for either the cosmological model or fundamental interactions, in particular when combined with CMB data (Planck).

Few examples:

- Non standard neutrino distribution in phase space
- Neutrino chemical potentials, i.e. neutrino-antineutrino (helicity) asymmetry
- Non standard lepton interactions
- Sterile neutrinos, dark radiation
- Decaying massive particles
- Low reheating at the Mev scale
- Massive particles in the MeV range or heavier
- Varying coupling constant
- Extra-dimensions
- …

# Non standard scenarios: degenerate ν?

BBN and CMB indirect probes of non-standard cosmological models. In particular, BBN is strongly sensitive to the expansion rate (Hubble parameter), and any departure from the standard scenario can show up in $N_{eff}$.

To break the degeneracy the $^4$He abundance is employed with two different $Y_p$ astrophysical measures, resulting in compatibility or tension of BBN with the Planck measure of the baryon density (the grey band is the 2-σ marginalized region from the Planck analysis with free $N_{eff}$).

Sykes et al, MNRAS 492 (2020) 2051

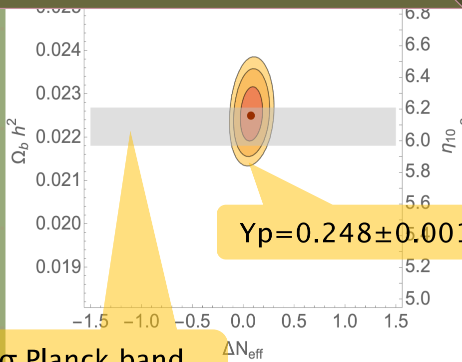


Matsumoto et al, arXiv:2203.09617 (2022)

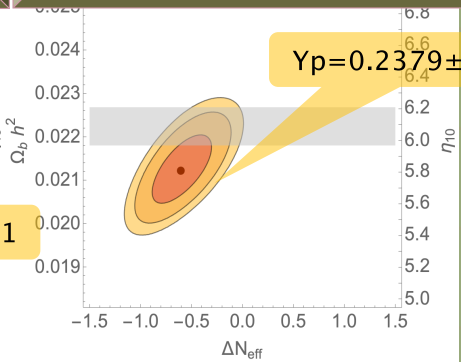


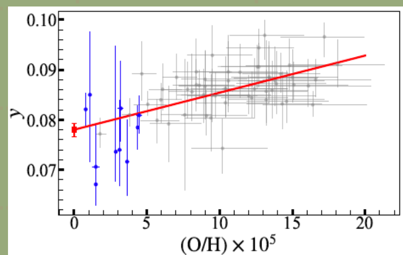

2−σ Planck band for free $N_{eff}$

# Non standard scenarios: degenerate ν?

BBN and CMB indirect probes of non-standard cosmological models. In particular, BBN is strongly sensitive to the expansion rate (Hubble parameter), and any departure from the standard scenario can show up in $N_{eff}$.

To break the degeneracy the $^4$He abundance is employed with two different $Y_p$ astrophysical measures, resulting in compatibility or tension of BBN with the Planck measure of the baryon density (the grey band is the 2-σ marginalized region from the Planck analysis with free $N_{eff}$).

Sykes et al, MNRAS 492 (2020) 2051

Matsumoto et al, arXiv:2203.09617 (2022)

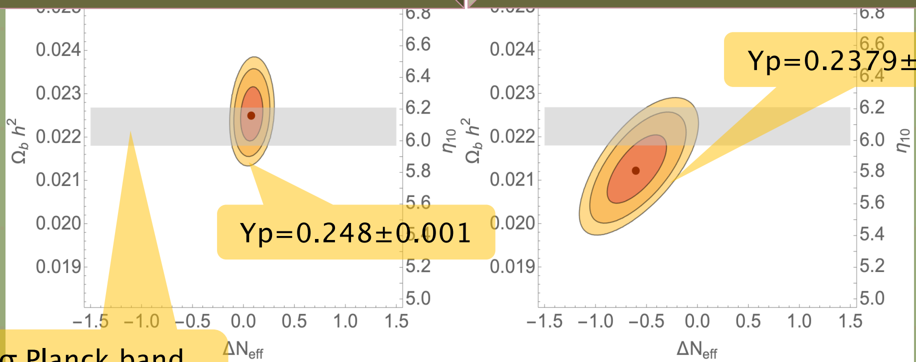


Yp=0.248±0.001

Yp=0.2379±0.0030

2−σ Planck band for free $N_{eff}$

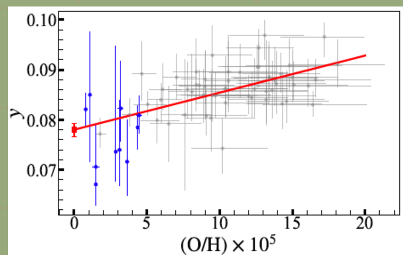


$$f_{eq}(p,T) = \frac{1}{e^{\frac{p}{T}-\frac{\mu_\nu}{T}}+1}$$

$$\xi_i \equiv \frac{\mu_{\nu_i}}{T}$$

degeneracy parameter, invariant under cosmic expansion

$$\Delta N_{eff}^{(\xi)} = \sum_i \left(\frac{30\xi_i^2}{7\pi^2} + \frac{15\xi_i^4}{7\pi^4}\right)$$

# Non standard scenarios: degenerate ν?

BBN and CMB indirect probes of non-standard cosmological models. In particular, BBN is strongly sensitive to the expansion rate (Hubble parameter), and any departure from the standard scenario can show up in $N_{eff}$.

To break the degeneracy the $^4$He abundance is employed with two different $Y_p$ astrophysical measures, resulting in compatibility or tension of BBN with the Planck measure of the baryon density (the grey band is the 2-σ marginalized region from the Planck analysis with free $N_{eff}$).

Sykes et al, MNRAS 492 (2020) 2051

Matsumoto et al, arXiv:2203.09617 (2022)

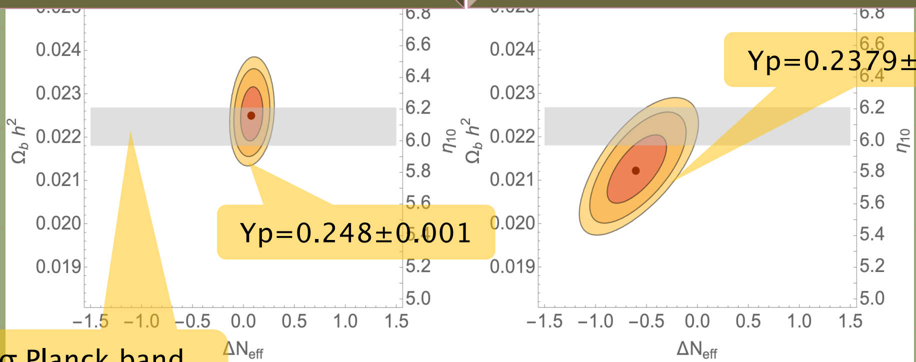


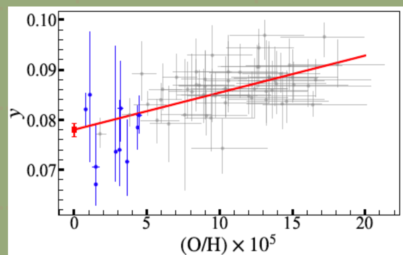


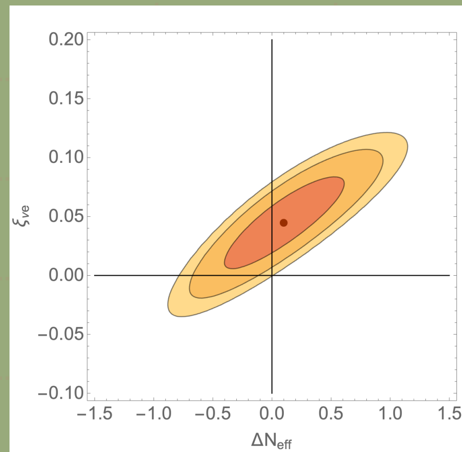


1-σ

$$f_{eq}(p,T) = \frac{1}{e^{\frac{p-\mu_\nu}{T}}+1}$$

$$\xi_i \equiv \frac{\mu_{\nu_i}}{T}$$

degeneracy parameter, invariant under cosmic expansion

$$\Delta N_{eff}^{(\xi)} = \sum_i \left( \frac{30\xi_i^2}{7\pi^2} + \frac{15\xi_i^4}{7\pi^4} \right)$$

$$\xi_{\nu e} = 0.046 \pm 0.025$$

$$N_{eff} = 3.14 \pm 0.33$$

# Non standard scenarios: degenerate ν?

Escudero et al., e-Print: 2208.03201

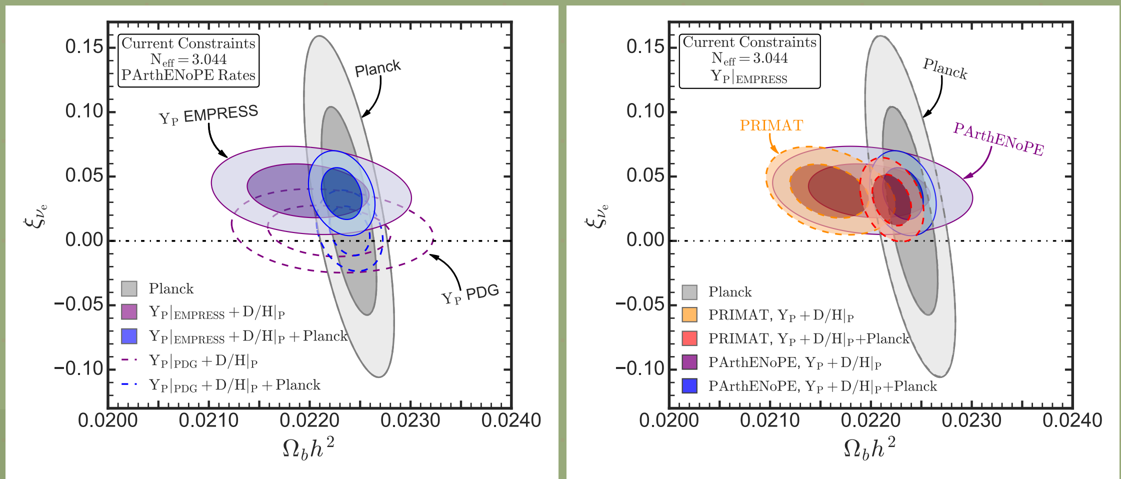


FIG. 2. 1 and $2\sigma$ C.L. regions for $\xi_{\nu_e}$ and $\Omega_b h^2$ from nucleosynthesis data, CMB data, and their combination for a cosmlogical scenario without dark radiation (*i.e.* assuming $N_{\rm eff} = N_{\rm eff}^{\rm SM} = 3.044$). The left panel compares the favored regions for two determinations of the helium abundance (EMPRESS survey and the PDG-21 recommended value) adopting the PArthENoPE nuclear rates, while the right panel compares the favored regions for two choices of the nuclear reaction rates (PArthENoPE or PRIMAT) adopting the EMPRESS measurement of the helium abundance.

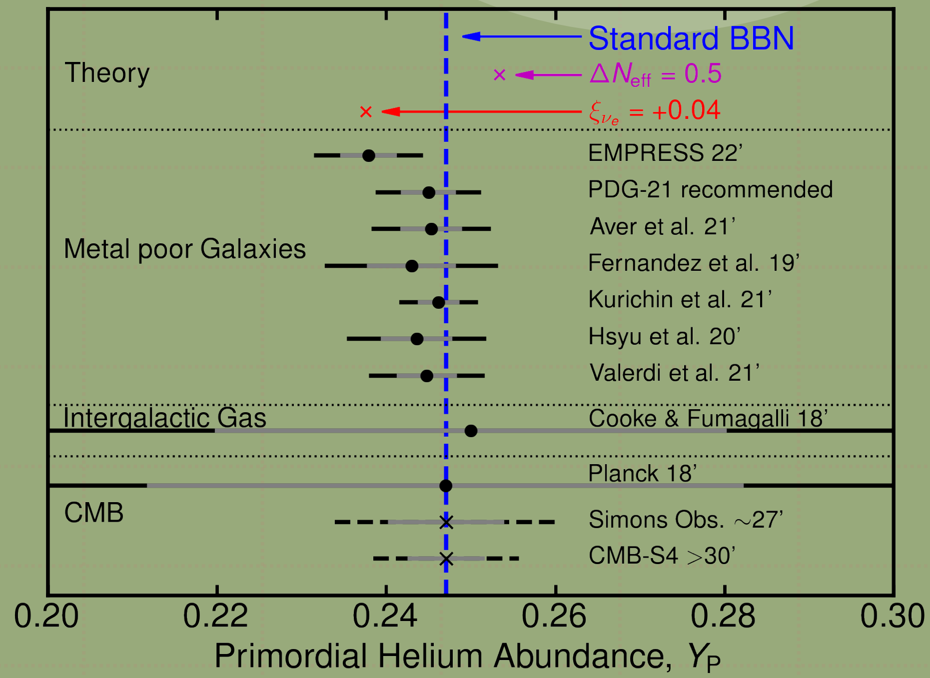

# Conclusions

- BBN, alone or combined with other cosmological probes (CMB, LSS,…) can constrain exotic physics beyond the Standard Model
- Presently, up to some claims of a 2 sigma level tension, the standard picture is consistent
- New astrophysical precise data are expected in the next years or so, maybe urging theorist to further improve the precision of the BBN predictions
- Nuclear physics input fundamental, both for the central value and the uncertainties of the prediction of primordial abundances. Focus has now shifted to DD transfer reactions, whose rates are responsible for different claims on the "health" of the cosmological model

# Thank you!

# Extra slides

# S-factor analysis

O.P. et al, JCAP 04 (2021) 020

Analyses differ for: data selection criteria and/or methods of analysis (R-matrix for resonances, empirical or nuclear theory inspired form for smooth S-factors, $\chi^2$, Bayesian, Monte Carlo, …). Our approach:

- Data: $E_{ik}$, $S_{ik}$, $\sigma_{ik}$, $\varepsilon_k$ (normalization uncertainty, if not given it is estimated as $\max[\sigma_{ik}/S_{ik}]$)
- Estimator: standard chi-squared plus a penalty factor: $$\chi^2(a_l, \omega_k) = \sum_{i_k} \frac{(S_{th}(E_{i_k}, a_l) - \omega_k\, S_{i_k})^2}{\omega_k^2\, \sigma_{i_k}^2} + \sum_k \frac{(\omega_k - 1)^2}{\epsilon_k^2}$$
- $S_{th}$ : empirical → polynomials (all data, even at high energy, for constraining the shape)
- Fit parameters: $a_l$, $\omega_k$ (the penalty factor disfavours $\omega_k$-1 to be greater than the normalization, $\varepsilon_k$)
- Standard error propagation: $$\Delta R^2(T) = \int_0^\infty \mathrm{d}E'\, K(E',T) \int_0^\infty \mathrm{d}E\, K(E,T) \sum_{i,j} \frac{\partial S_{\mathrm{th}}(E',a)}{\partial a_i}\bigg|_{\widehat{a}} \frac{\partial S_{\mathrm{th}}(E,a)}{\partial a_j}\bigg|_{\widehat{a}} \mathrm{cov}(a_i,a_j).$$
- Final uncertainty combining the inflated ΔR with an overall scale error η

$$\delta R^2 = \chi^2_{red} \Delta R^2 + \eta^2$$

$$\eta^2 = \sum_k \frac{(\omega_k - 1)^2}{\chi^2_{k,red}} \Bigg/ \sum_k \frac{1}{\chi^2_{k,red}}$$

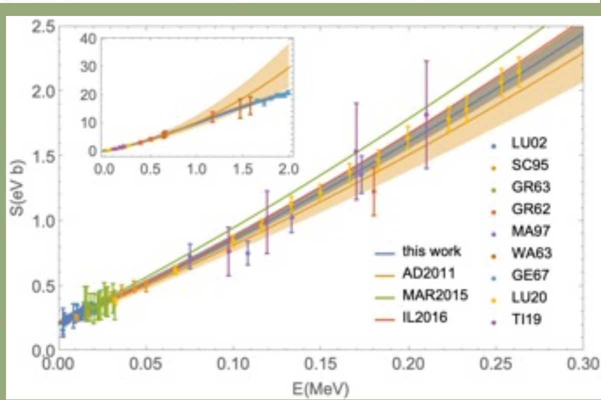

O.P. et al, JCAP 04 (2021) 020

# Sensitivities

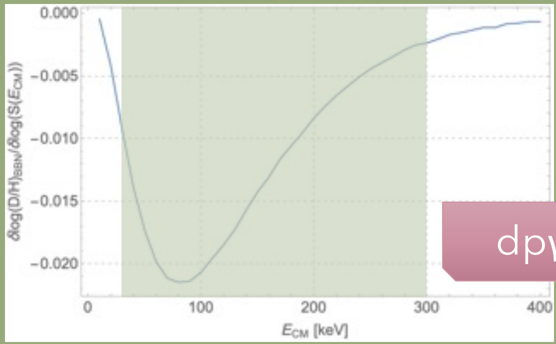


dpγ

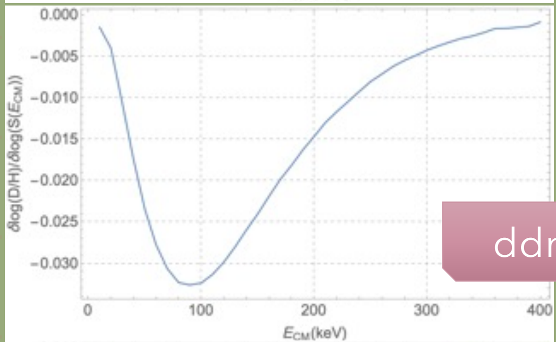


ddn

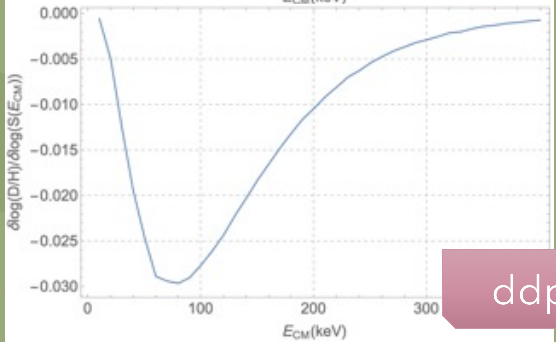


ddp

We change the S-factor of δS at a given energy Ecm and observe the corresponding variation in the deuterium yield δ(D/H).

The sensitivity defined as (Fiorentini et al. 1998, Nollett and Burles 2000)

$$\sigma(E_{CM}) = \frac{\delta(D/H)/(D/H)}{\delta S(E_{CM})/S(E_{CM})}$$

For the three deuterium reactions the BBN relevant range is ~ 10-400 keV with a maximum at ~ 80 keV.

# Deuterium

1. Determination of D/H at high redshift help ensure that the observed abundance is close to primordial one.
2. From a set of five high quality absorbers it was determined $^{2}H/H=(2.53\pm0.04)\cdot10^{-5}$ (R. Cooke et al., *Astrophys.J.* 781 (2014) 31.
3. A measure $^{2}H/H=(2.45\pm0.28)\cdot10^{-5}$ at z=3.256 remains debated (S. Reimer-Sorensen et al., *MNRAS* 447 (2015) 2925).
4. After recent new observations or reanalyses of existing data the new value, with 1.2% uncertainty, is $^{2}H/H=(2.527\pm0.030)\cdot10^{-5}$ (R. Cooke et al., *Astrophys.J.* 855 (2018) 102).
5. The weighted mean of the latest 11 measures gives $^{2}H/H=(2.55\pm0.03)\cdot10^{-5}$ (B.D. Fields et al., *JCAP* 03 (2020) 010).
6. Very promising improvement foreseen in the measure by 30 m class telescopes.

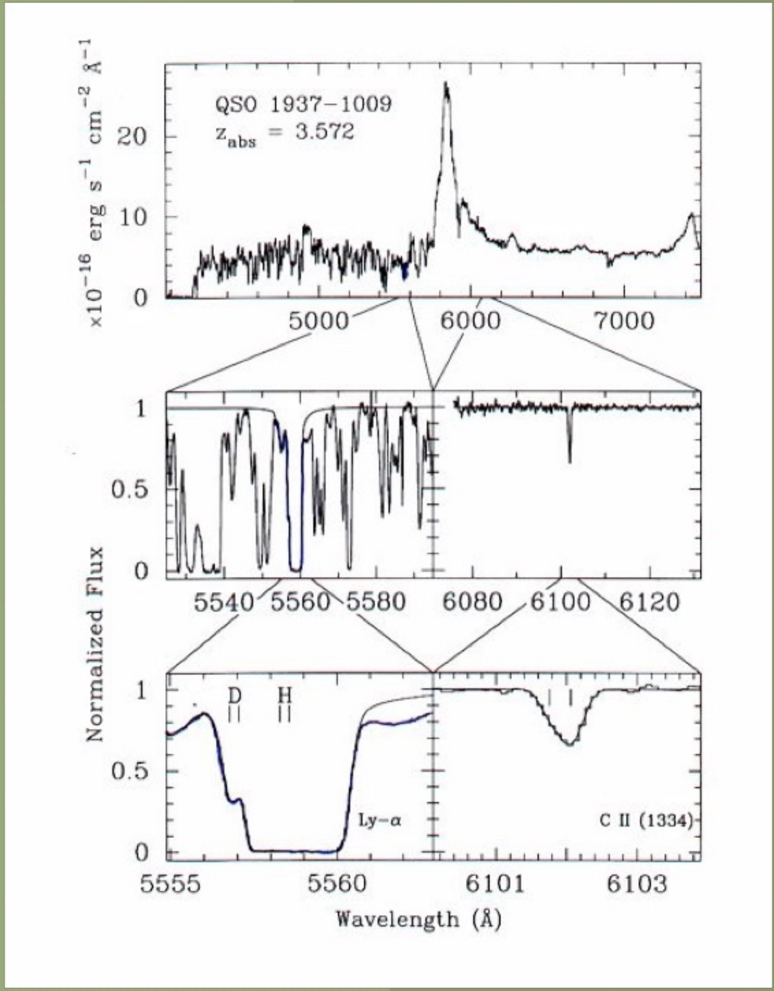

# Helium

1. The theoretical model used for extracting the abundance contains several physical parameters (among which $^4$He abundance, electron density, optical depth, temperature, neutral H fraction). However, there was a degeneracy between the electron density and the temperature of the gas.
2. More recently, the near-infrared (NIR) line HeIλ10830 was included in the analysis, which is key to removing such a degeneracy.
3. From the study of 54 galaxies (three of which are Extremely Metal Poor Galaxies, EMPGs, less than 10% of solar metallicity), it results $Y_p$=0.2436±0.0040 (T. Hsyu et al, *Astrophys.J.* 896 (2020) 77).
4. An alternative method consists in studying intergalactic absorption lines in almost primordial clouds between us and a background quasar, from which $Y_p$=0.250±0.033 (C. Sykes et al, *MNRAS* 492 (2020) 2151). Same authors give $Y_p$=0.248±0.001 as a weighted average of all recent determinations.
5. Adding to the sample 10 EMPGs, a new results was released recently, $Y_p$=0.2379±0.0030 (A. Matsumoto et al, e-Print: 2203:09617).
6. Promising measurement from the damping tail of the CMB acoustic peak, for the moment not competitive with astrophysical measure.

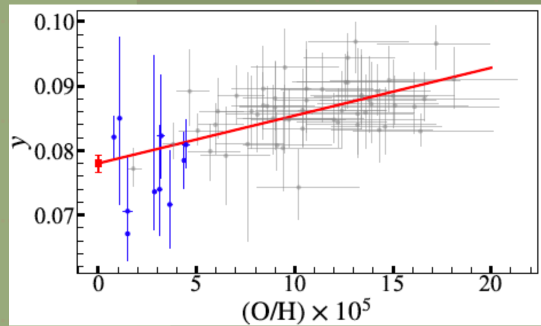


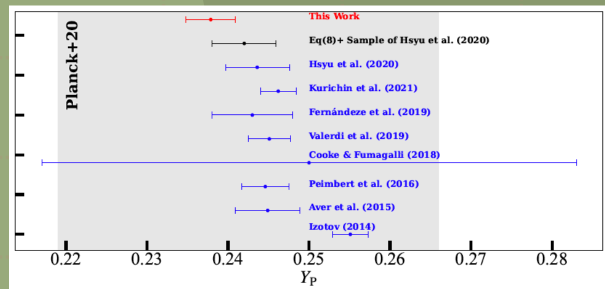


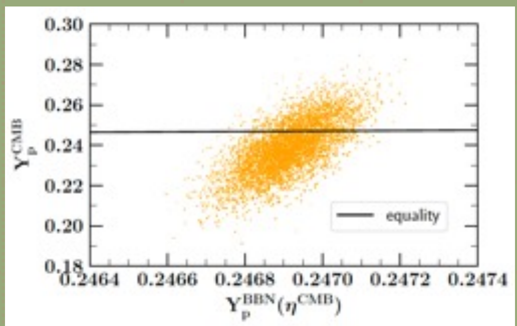

# Lithium-6 problem

Asplund et al, ApJ 644 (2006) 229

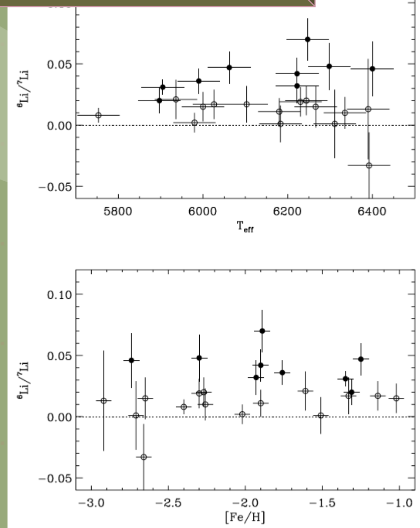


1. Lithium is the only element with three production channels: BBN, CR, and stars.
2. First observations (1995-1997) of $^7$Li in low metallicity halo stars consistent with the existence of Spite plateau, justifying its association with the primordial $^7$Li abundance.
3. High precision astrophysical data on D/H (1998), confirmed by CMB measurement of $\Omega_b h^2$, predicted a $^7$Li/H abundance in excess of this plateau value, the primordial $^7$Li problem.
4. The lack of dispersion in the $^7$Li abundance data was initially the argument against a possible depletion of $^7$Li in stars with lower surface temperatures or higher metallicities. But first indications of a departure from the $^7$Li plateau (2010) and significant dispersion at low metallicity in more recent works (2018-2021) points to stellar depletion processes.
5. Any depletion in $^7$Li should imply at least as much depletion in $^6$Li, but initial observations (1998) of $^6$Li in halo stars was entirely consistent with expected ($^6$Li/$^7$Li ~ $10^{-5}$).
6. Several years after (2006), measurements of $^6$Li in some very metal-poor dwarfs indicated an abundance about a thousand times that predicted ($^6$Li/$^7$Li ~ $10^{-2}$), the primordial $^6$Li problem.
7. The reality of a $^6$Li plateau could not be established because its detection is based on delicate fits to the line shape. Moreover, stars with sizable values of $^6$Li are close to the main-sequence turn-off in the HR diagram, i.e. the hottest stars of the sample.
8. A very recent (2022) measure of the isotopic ratio $^6$Li/$^7$Li in three Spite plateau stars, using refined star models and numerical methods with data from ESPRESSO/Very Large Telescope spectrograph, reports no $^6$Li in any of the three stars → no primordial $^6$Li problem.

Wang et al, Mon.Not.Roy.Astron.Soc. 509 (2021) 1, 1521

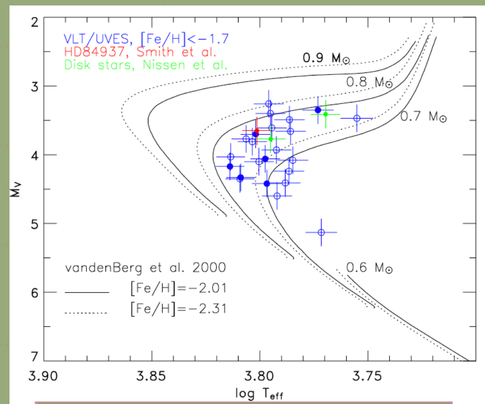


Lambert, AIP Conf.Proc. 743 (2004) 1, 206